JCIS-12-2208 Revised December 2012

Block copolymer-mediated synthesis of gold nanoparticles in aqueous solutions: Segment effect on gold ion reduction, stabilization and particle morphology

Toshio Sakai,[1*] Yuya Horiuchi,[1] Paschalis Alexandridis,[2] Tomohiko Okada,[1] and Shozi Mishima[1]

[1]Department of Chemistry and Material Engineering, Faculty of Engineering, Shinshu University, 4-17-1 Wakasato, Nagano 380-8553, Japan

[2]Department of Chemical and Biological Engineering, University at Buffalo, The State University of New York (SUNY), Buffalo, NY 14260-4200, USA

* To whom correspondence should be addressed.

Phone: +81-26-269-5405

Fax: +81-26-269-5424

E-mail: tsakai@shinshu-u.ac.jp

Abstract

We report here on the segment effects of poly(ethylene oxide)-containing block copolymers (PEO-BCP) on the reduction activity for tetrachloride gold(III) ($[AuCl_4]^-$), interfacial activity for gold surface, colloidal stability and morphology of gold nanoparticles formed in aqueous solutions. In particular, the effects of poly(ethylene oxide) (PEO), poly(propylene oxide) (PPO), polyethylene (PE) segments and amino group (NH_2) on the rate of $[AuCl_4]^-$ reduction, adsorption of PEO-BCP onto gold surface, colloidal stability and morphology of gold nanoparticles formed in aqueous solutions were examined using a poly(ethylene oxide)-poly(propylene oxide) triblock copolymer (PEO-PPO-PEO, Pluronic L44), an amino-terminated poly(ethylene oxide)-poly(propylene oxide) block copolymer (PEO-PPO-NH_2, SURFONAMINE® L-207), a poly(ethylene oxide) homopolymer (PEO, Poly(ethylene glycol)2000), and a polyethylene-poly(ethylene oxide) block copolymer (PE-PEO, Polyethylene-block-poly(ethylene glycol)). We found that the reduction activity of PEO-BCP for $[AuCl_4]^-$ became higher with the order of PEO-PPO-NH_2 < PE-PEO < PEO < PEO-PPO-PEO. The interfacial activity (affinity) of PEO-BCP for gold surface increased with the order of PEO < PE-PEO < PEO-PPO-PEO << PEO-PPO-NH_2. Consequently, the colloidal stability of gold nanoparticles formed in aqueous PEO-PPO-NH_2 solutions was extremely high compared with that in PEO, PEO-PPO-PEO and PE-PEO solutions. In addition, the size of gold nanoparticles formed in aqueous PEO-PPO-NH_2 solutions was much smaller than that in aqueous solutions of PEO-PPO-PEO, PEO or PE-PEO.

Keywords: Poly(ethylene oxide)-containing block copolymer; Gold nanoparticles; Reduction activity; Interfacial activity; Colloidal stability; Particle morphology

1. Introduction

Nanometer-scale gold particles (gold nanoparticles) have attracted significant attention in the last couple of decades because of their unique properties that are distinct from bulk gold [1-11]. In addition, the size, shape and assembly of gold nanoparticles are extremely important features because they substantially affect the physical and chemical properties of the nanoparticles. Therefore, the controllable synthesis of gold nanoparticles with different sizes, shapes and assemblies still remains a very important and challenging issue.

The size, shape and assembly of gold nanoparticles are controlled by judicious combination of the capping agents (e.g., alkylthiols, surfactants and polymers) and reducing agents (e.g., $NaBH_4$, hydrazine and ascorbic acid). There are a number of reports on the utilization of organic thiols as capping agents for gold nanoparticles including the pioneering work done by Brust et al. [12]. On the other hand, the block copolymer- and supramolecule-mediated synthesis of gold nanoparticles has been recently developed because the block copolymers and supramolecules can display dual function: the reducing function for metal ions and capping (stabilizing) function for metal nanoparticles formed [13-15]. For example, amino-terminated block copolymers [16-20], amine-functionalized dendrimers [21], 3-thiophenemalonic acid [22], 3-heptadecafluoroctylsulfonyaminopropyltrimethylammonium iodide [23], poly(ethylene glycol) [24], poly(ethylene oxide)-poly(propylene oxide) (PEO-PPO) block copolymers [25-31] and poly(ethylene oxide)-containing block copolymers [32-35] have achieved the one-step synthesis and stabilization of gold nanoparticles formed from tetrachloride gold(III) ($[AuCl_4]^-$) in aqueous solutions in the absence of additional reductant (e.g., sodium borohydride, hydrazine and citric acid) and energy

input (e.g., photo- and ultrasound-irradiation) for the $[AuCl_4]^-$ reduction. We have also demonstrated that the PEO-containing block copolymers (PEO-BCP) such as PEO-PPO block copolymers [25-29], amino-terminated PEO-PPO block copolymers [19, 20] and poly(ethylene glycol)-grafted phospholipids [35] can act as efficient reducing and stabilizing agents in the one-step synthesis and stabilization of gold nanoparticles in air-saturated aqueous solutions at ambient temperature in the absence of additional reductant and energy input for the $[AuCl_4]^-$ reduction. The block copolymer-mediated synthetic method provides advantages in the environmental and economical aspect since the synthetic method requires a simple procedure which is the mixing of metal salt with a block copolymer solution. Also the methodology of block copolymer-mediated metal nanoparticle synthesis offers various possibilities (e.g., variation of block copolymer type, amphiphilic character, concentration, temperature, solvent) to control the size, shape and colloidal stability of metal nanoparticles. However, the roles of the block copolymer for the reduction of metal ions and control of size, shape and colloidal stability of metal nanoparticles formed in solutions are still not clarified. Therefore, we should obtain a better insight on the reducing and stabilizing functions of block copolymer, and understand the full potential of the block copolymers for further development of the block copolymer-mediated synthesis of metal nanoparticles. In particular, the role of block copolymer segment for the reduction of metal ions and control of size, shape and colloidal stability of metal nanoparticles formed should be evaluated because each segment of block copolymer could exhibit the particular function such as the reducing- and anchoring-function.

In the present work, we examine the gold nanoparticles synthesis from the reduction of $[AuCl_4]^-$ using a poly(ethylene oxide)-poly(propylene oxide) triblock

copolymer (PEO-PPO-PEO), an amino-terminated poly(ethylene oxide)-poly(propylene oxide) block copolymer (PEO-PPO-NH_2), a poly(ethylene oxide) homopolymer (PEO) and a polyethylene-poly(ethylene oxide) block copolymer (PE-PEO) in aqueous solutions in order to evaluate the effect of PEO, PPO, PE blocks and NH_2 on the $[AuCl_4]^-$ reduction, particle growth, stabilization and morphology of gold nanoparticles formed.

2. Experimental

2.1 Preparation of Gold Nanoparticles

Gold nanoparticles were prepared by mixing of an aqueous hydrogen tetrachloroaurate (III) hydrate ($HAuCl_4 \cdot 4H_2O$, 99.9+ %; Wako) solution and a 5.0×10^{-3} mol L^{-1} aqueous polymer solution containing a poly(ethylene oxide)-poly(propylene oxide)-poly(ethylene oxide) block copolymer (PEO-PPO-PEO) (Pluronic L44, $H[OCH_2CH_2]_{10}[OCH_2CH(CH_3)]_{23}[OCH_2CH_2]_{10}OH$, FW2200, BASF Corp.), an amino-terminated poly(ethylene oxide)-poly(propylene oxide) block copolymer (PEO-PPO-NH_2) (SURFONAMINE® L-207, $CH_3[OCH_2CH_2]_{33}[OCH_2CH(CH_3)]_{10}NH_2$, FW2000, HUNTSMAN) (SURFONAMINE® L-207 was gifted from Mitsui Fine Chemicals, Inc.), a poly(ethylene oxide) homopolymer (PEO) (Poly(ethylene glycol)2000, $H[OCH_2CH_2]_{45}OH$, FW2000, Aldrich) and a polyethylene-poly(ethylene oxide) block copolymer (PE-PEO) (Polyethylene-block-poly(ethylene glycol), $CH_3CH_2[CH_2CH_2]_{14}[OCH_2CH_2]_{40}OH$, Aldrich). Concentration of $[AuCl_4]^-$ in the solutions was 0.2×10^{-3} mol L^{-1} at the reaction initiation. Ultrapure water (18.2 MΩ cm at 25 °C, Millipore-filtered water) was used in all experiments. Following agitation by vortex mixer for ~10 sec, the solutions were left standing at a given

temperature (20, 40, 60 and 80 °C) for the reaction to proceed.

2.2 Characterization

The reduction of $[AuCl_4]^-$ and the formation of gold nanoparticles were monitored by observing changes in the absorption spectra centered at ~220 nm originating from $[AuCl_4]^-$ [25, 26] and those centered at ~540 nm originating from the surface plasma resonance (SPR) of the gold nanoparticles [36, 37] using a UV-visible spectrophotometer (U-1900, HITACHI).

The size and shape of the obtained gold nanoparticles were determined by a transmission electron microscope (TEM) (JEM-2010, JEOL Ltd.) in conventional transmission mode using 200 kV. TEM observation was carried out at the point when the reaction completed. Thus, the points (reaction times) of TEM observation are different in the every sample. The reaction completion was judged from the plateau region of the time course changes in the $Abs._{Max}$@$[AuCl_4]^-$ (see upper panel of **Figure 2**).

The interfacial activity (affinity) of block copolymers for gold surface was determined by measuring the amount of polymers adsorbed on quartz crystal resonator with gold electrode (QA-A9M-AU(M), SEIKO EG&G Co., Ltd.) with a quartz crystal microbalance (QCM) (QCM934 system, SEIKO EG&G Co., Ltd.) at 25 °C.

3. Proposed mechanism on $[AuCl_4]^-$ reduction and gold nanoparticle formation

It is considered that the formation of gold nanoparticles from $[AuCl_4]^-$ in the PEO-containing block copolymer (PEO-BCP) aqueous solutions includes three main steps [26].

Step 1 (Nucleation): Reduction of $[AuCl_4]^-$ by PEO-BCP.

The PEO-BCP forms pseudocrown ether structures (cavities) with $[AuCl_4]^-$:

$$[AuCl_4]^- + n\text{PEO-BCP} \rightarrow [AuCl_4]^-\text{-(PEO-BCP)}_n \quad (1)$$

where $[AuCl_4]^-$-$(\text{PEO-BCP})_n$ represents $[AuCl_4]^-$ bound to cavities that are formed from PEO coils [38-40]. Reduction of bound $[AuCl_4]^-$ proceeds via oxidation of the polymer by the metal center [24].

$$[AuCl_4]^-\text{-(PEO-BCP)}_n \rightarrow Au^0 + 4Cl^- + 2H^+ + \text{oxidation products} \quad (2)$$

Carboxylate groups have been identified as oxidation products by FT-IR in PEO homopolymer systems [24] after $[AuCl_4]^-$ reduction.

Step 2 (Growth): Absorption of block copolymers on the surface of gold clusters and reduction of $[AuCl_4]^-$ in that vicinity.

Block copolymers adsorb on the surface of gold clusters, $(Au^0)_m$, formed through reduction of $[AuCl_4]^-$ in solution, due to the interfacial activity of the PEO-BCPs.

$$(Au^0)_m + l\text{PEO-BCP} \rightarrow (Au^0)_m\text{-(PEO-BCP)}_l \quad (3)$$

where $(Au^0)_m$-$(\text{PEO-BCP})_l$ represents a gold cluster with adsorbed block copolymers. The adsorbed block copolymers can form pseudocrown ether structures that bind with

$[AuCl_4]^-$, $(Au^0)_m$-(PEO-BCP)$_l$-$[AuCl_4]^-$, and facilitate their reduction. The reduction of $[AuCl_4]^-$ and formation of gold clusters is repeated on the surface of gold nanoparticles, and therefore the particles grow.

Step 3 (Stabilization): Stabilization of gold nanoparticles by block copolymers

The reduction of $[AuCl_4]^-$ is completed and the resulting gold nanoparticles are stabilized by block copolymers.

4. Results and Discussion

4.1 Effect of block copolymer segment on reduction of $[AuCl_4]^-$

We first examine the connection between block copolymer segment and reduction activity of PEO-BCP for $[AuCl_4]^-$. The $[AuCl_4]^-$ reduction was confirmed by monitoring the decrease in the absorbance centered at ~220 nm originating from the $[AuCl_4]^-$ with elapsed time after mixing of an aqueous $[AuCl_4]^-$ solution with an aqueous PEO-BCP solution (see **Figure 1**). Correspondingly, the absorbance centered at ~540 nm originating from SPR of the gold nanoparticles increased with the elapsed time (see inset of **Figure 1**).

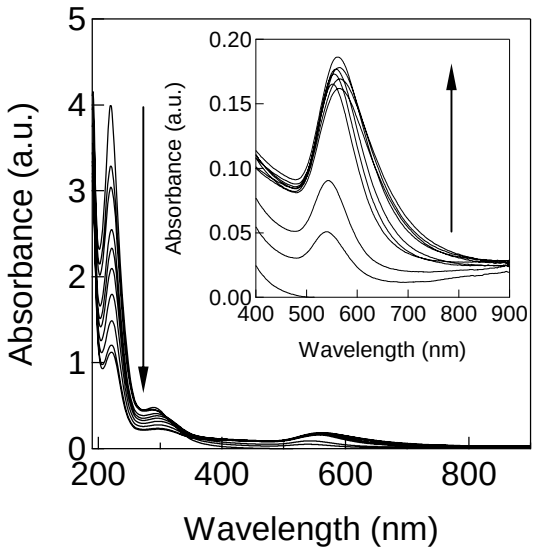

Figure 1. Absorption spectra centered at ~220 nm originating from $[AuCl_4]^-$ in aqueous PEO-PPO-PEO solutions at 20 ˚C recorded as a function of elapsed time. The inset shows a change in the absorption spectra centered at ~540 nm from SPR of gold nanoparticles formed. The arrows represent the direction of time course changes in the absorption spectra.

The maximum absorbance at ~220 nm originating from $[AuCl_4]^-$ ($Abs._{Max}$@$[AuCl_4]^-$) was plotted as a function of elapsed time (see upper panel of **Figure 2**). The $Abs._{Max}$@$[AuCl_4]^-$ decreased gradually up to 360 h (15 d) in an aqueous PEO-PPO-PEO solution at 20 °C after reaction initiation. The rate of decrease of $Abs._{Max}$@$[AuCl_4]^-$ became faster with higher temperature (see upper panel of **Figure 2**). This trend was observed in every PEO-BCP that we examined in this work. Namely, the $[AuCl_4]^-$ reduction in aqueous block copolymer solutions was promoted by temperature elevation. Note here that no significant decrease in the absorbance originating from $[AuCl_4]^-$ and no SPR band of gold nanoparticles were observed for the aqueous solution containing 0.2×10^{-3} mol L^{-1} $[AuCl_4]^-$ (no polymer

solution) in the temperature range of 20-80 °C for 480 h (20 d) that we monitored. We also observed an increase in maximum absorbance at ~540 nm originating from SPR of gold nanoparticles ($Abs._{Max}$@SPR) at early stage of the reaction and decrease in the $Abs._{Max}$@SPR with the elapsed time after $Abs._{Max}$@SPR reached to maximum (see bottom panel of **Figure 2**). The increase in $Abs._{Max}$@SPR at the early stage of the reaction corresponds to the nucleation and growth of gold nanoparticle. The rate of the increase in $Abs._{Max}$@SPR at early stage of the reaction became faster with higher temperature. This indicates that the formation of gold nanoparticles is promoted by temperature elevation. This heating-enhanced particle formation induced the precipitation of gold nanoparticles in solutions. As shown in **Figures 4 and 5,** the stabilizing function of PEO-PPO-PEO, PEO and PE-PEO for gold nanoparticles formed in aqueous solutions is low so that gold nanoparticles formed in aqueous solutions containing PEO-PPO-PEO, PEO and PE-PEO precipitate in the solutions. As a result, $Abs._{Max}$@SPR decreased with elapsed time after $Abs._{Max}$@SPR reached to maximum. The rate of the decrease in $Abs._{Max}$@SPR increased with higher temperature. Namely, faster formation of gold nanoparticles with higher temperature leads to the faster precipitation of gold nanoparticles formed.

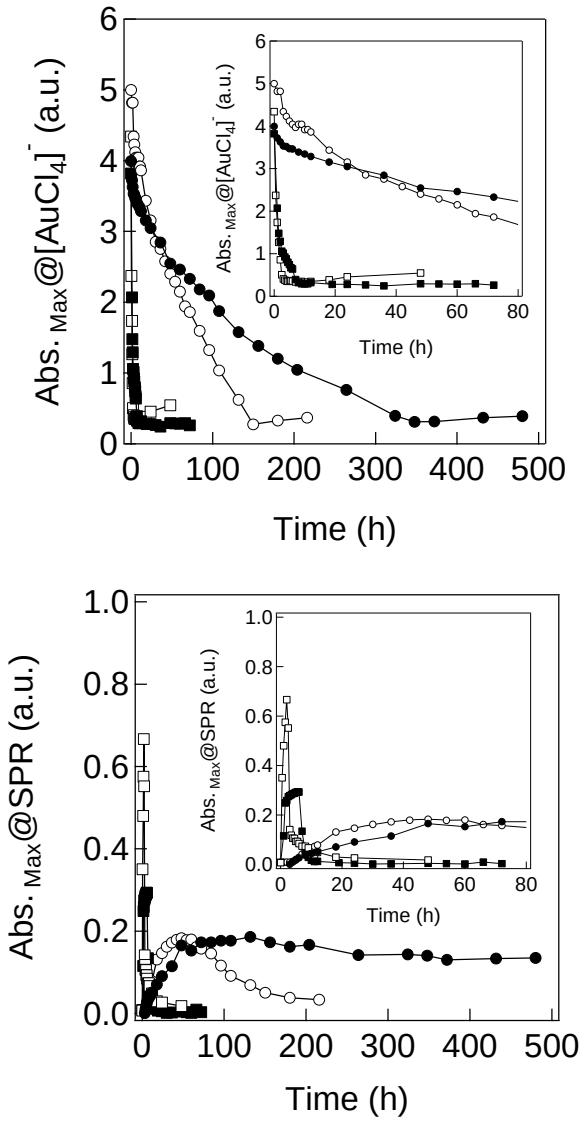

Figure 2. (Upper panel) Maximum absorbance at ~220 nm ($Abs._{Max}@[AuCl_4]^-$) originating from $[AuCl_4]^-$ and (Lower panel) maximum absorbance at ~540 nm ($Abs._{Max}$@SPR) originating from SPR of gold nanoparticles plotted as a function of the elapsed time after mixing aqueous $[AuCl_4]^-$ solution and aqueous PEO-PPO-PEO block copolymer at 20 ˚C (●), 40 ˚C (○), 60 ˚C (■), and 80 ˚C (□). The inserts show the time evolutions of $Abs._{Max}@[AuCl_4]^-$ and $Abs._{Max}$@SPR at the early stage of reaction (0-80 h).

On the basis of the mechanism proposed in section 3, the kinetics of $[AuCl_4]^-$ reduction were considered in order to evaluate the connection between block copolymer segment and reduction activity of PEO-BCP for $[AuCl_4]^-$. Reaction (1) is considered the kinetically dominant process in the initial stage of $[AuCl_4]^-$ reduction, so the reduction rate of $[AuCl_4]^-$ is given by:

$$-d[AuCl_4^-]/dt = k[AuCl_4^-][PEO\text{-}BCP]^n \quad (4)$$

$$[AuCl_4^-] = [AuCl_4^-{}_0]\exp\{-k[PEO\text{-}BCP]^n t\} \quad (5)$$

where $[AuCl_4^-]$ is the $[AuCl_4]^-$ concentration and [PEO-BCP] is the block copolymer concentration participating in the reaction. $[AuCl_4^-{}_0]$ is the initial concentration of $[AuCl_4]^-$, and k is the reduction rate constant. The time course change of the $[AuCl_4]^-$ concentration is given by:

$$[AuCl_4^-] = [AuCl_4^-{}_0]\exp\{-K t\} \quad (6)$$

$$K = k[PEO\text{-}BCP]^n \quad (7)$$

where K denotes the apparent rate constant of the reduction.

The apparent rate constant, K, thus estimated was plotted in **Figure 3** as a function of temperature. The apparent rate constant, K, was larger with the order of PEO-PPO-NH_2 < PE-PEO < PEO < PEO-PPO-PEO in the temperature range of 20-80 °C that we examined (see **Figure 3**). This indicates that the reduction activity of

block copolymer for $[AuCl_4]^-$ becomes higher with the order of PEO-PPO-NH_2 < PE-PEO < PEO < PEO-PPO-PEO. Namely, the PPO segment in block copolymer enhances the reduction of $[AuCl_4]^-$, while PE and NH_2 prevent the $[AuCl_4]^-$ reduction.

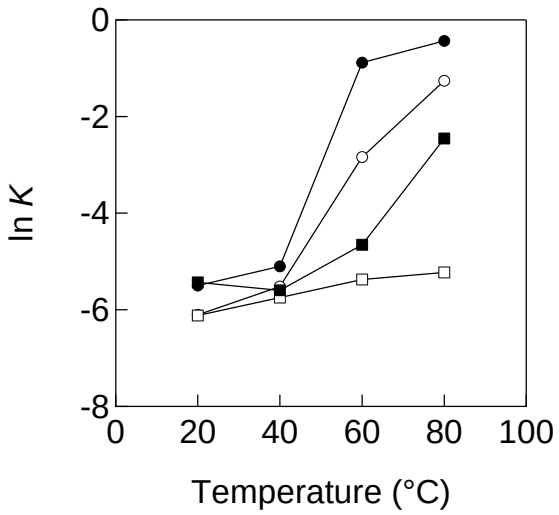

Figure 3. Apparent rate constant (K) of $[AuCl_4]^-$ reduction by polymers: PEO-PPO-PEO (●), PEO-PPO-NH_2 (□), PEO (○) and PE-PEO (■).

We consider that the reduction activity of PEO-BCP for $[AuCl_4]^-$ is attributed to (i) PEO-BCP conformation or structure (e.g., loops vs. entanglements, or non-associated polymers vs. micelles) and (ii) interactions between $[AuCl_4]^-$ and PEO-BCP (attractive ion-dipole interactions vs. repulsive interactions due to hydrophobicity) [26, 27]. The higher reduction activity of PEO-PPO-PEO than that of PEO homopolymer suggests that micelle formation is related to the reduction activity of PEO-BCP for $[AuCl_4]^-$. The reduction of $[AuCl_4]^-$ in the aqueous PEO-BCP solutions is responsible for the formation of pseudocrown ether structures (cavities) of PEO segment with $[AuCl_4]^-$ [26, 27]. Namely, the formation of PEO loops (cavities) should be related to the activity of

PEO-BCP for $[AuCl_4]^-$ reduction. The formation of PEO loops (cavities) is attributed to PEO-BCP conformation and structure (e.g., non-associated polymers, aggregates and micelles) [26, 27]. For example, if polymers formed aggregates, the formation of polymer loops (cavities) would be prevented by entanglement. Since PEO homopolymers form aggregates, the formation of PEO loops (cavities) would be prevented in the aggregates due to the entanglement. On the other hand, PEO-PPO-PEO in the micelles would produce a number of PEO loops (cavities) in the micelle corona which act as reaction sites (surface cavities) for $[AuCl_4]^-$ reduction because a micelle involves well-ordered structure of block copolymers (without entanglement among block copolymers) [26, 27, 30, 31]. Low activity of PE-PEO for $[AuCl_4]^-$ reduction would be caused by polymer entanglement and repulsive interaction between $[AuCl_4]^-$ and PE-PEO due to the polymer hydrophobicity [27]. The lowest reduction activity of PEO-PPO-NH_2 observed in our experimental system is most likely due to the strong interaction among PEO-PPO-NH_2 afforded by hydrogen bonding. It is known that alkylamines bind each other by hydrogen bonding of amino groups [41]. In particular, PEO-PPO-NH_2 containing the primary amines make strong hydrogen bonding [41], and the strong hydrogen bonding among amino groups would prevent the ion-dipole interaction between $[AuCl_4]^-$ and PEO.

4.2 Effect of block copolymer segment on stabilization of gold nanoparticles formed

In general, the adsorption of surfactants and amphiphilic polymers on the surface of a growing particle limits the particle growth [42]. At the same time, the adsorption of surfactants and amphiphilic polymers on the particle surface contributes to

the colloidal stabilization of particles in solutions. We found that the amount of block copolymers adsorbed on gold surface in aqueous solutions (measured with QCM system) increased with the order of PEO < PE-PEO < PEO-PPO-PEO << PEO-PPO-NH_2 (see **Table 1**).

Table 1. Amount of polymers adsorbed on gold surface

Polymer	**Amount of polymers adsorbed on gold surface (10^{-7} mol cm^{-2})**
PEO-PPO-PEO	3.16
PEO-PPO-NH_2	6.46
PEO	1.60
PE-PEO	2.56

This indicates that the interfacial activity (affinity) of block copolymers for gold surface in aqueous solutions increases with the order of PEO < PE-PEO < PEO-PPO-PEO << PEO-PPO-NH_2. In particular, the amount of PEO-PPO-NH_2 adsorbed onto gold surface was more than twice than that of PEO-PPO-PEO, PEO and PE-PEO. The strong affinity and the resulting adsorption of PEO-PPO-NH_2 onto gold surface led to the high colloidal stability of gold nanoparticles in aqueous solutions. Clear red color of solutions and strong SPR originating from gold nanoparticles were observed only in the aqueous PEO-PPO-NH_2 solutions after reaction completed, while less red color solutions and weak SPR of gold nanoparticles were observed in the PEO-PPO-PEO, PEO and PE-PEO system (see **Figures 4 and 5**). That is, the gold nanoparticles formed in the aqueous PEO-PPO-NH_2 solutions remained well dispersed. The above obviously indicate that the affinity of an amino group with gold surface results in superior colloidal stability of gold nanoparticles in solutions.

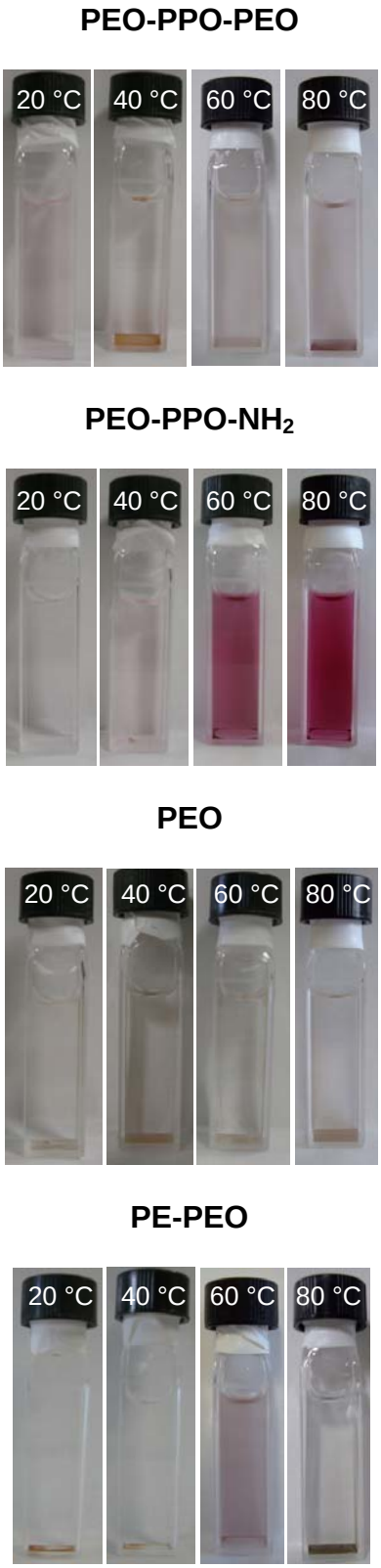

Figure 4. Colloidal stability of gold nanoparticles formed in aqueous polymer solutions.

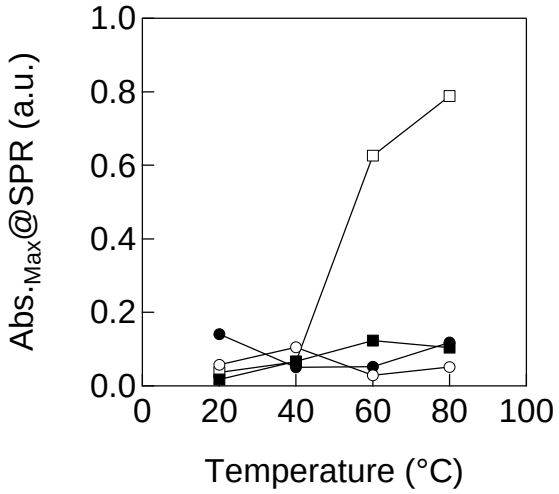

Figure 5. Maximum absorbances at ~540 nm ($Abs._{Max}$@SPR) from SPR of gold nanoparticles formed in aqueous polymer solutions at 20, 40, 60 and 80 ˚C: PEO-PPO-PEO (●), PEO-PPO-NH_2 (□), PEO (○) and PE-PEO (■).

4.3 Effect of block copolymer segment on morphology of gold nanoparticles formed

In the conventional method of metal nanoparticle synthesis, the adsorption of surfactants and amphiphilic polymers onto particle surface due to their interfacial activity (affinity) restricts the particle growth [42]. In contrast, the adsorption of PEO-BCP onto particle surface contributes to the particle growth in the block copolymer-mediated synthesis of gold nanoparticles presented here because PEO-BCP adsorbed on the gold seeds enables to reduce $[AuCl_4]^-$ in the vicinity of particle surface [26]. Namely, both the reduction activity and interfacial activity (affinity) of block copolymers must be taken into account for the determination of the particle growth and the resulting morphology of gold nanoparticles. From the reduction activity of block copolymers for $[AuCl_4]^-$ reduction and interfacial activity (affinity) of block copolymers for gold surface, the PEO-PPO-PEO system is expected to produce larger particles

because $[AuCl_4]^-$ should be reduced in the vicinity of gold surface by PEO-PPO-PEO adsorbed on the gold seeds due to the highest reduction activity for $[AuCl_4]^-$ and relatively high interfacial activity (affinity) for gold surface. On the other hand, the PEO-PPO-NH_2 system is expected to form smaller particles because the stabilization of gold nanoparticles by PEO-PPO-NH_2 should be significant compared with the $[AuCl_4]^-$ reduction by PEO-PPO-NH_2 in the vicinity of gold surface due to the lowest reduction activity for $[AuCl_4]^-$ and the highest interfacial activity (affinity) for gold surface in the polymers that we examined in this work. Indeed, gold particles with a diameter in the range 80-300 nm were formed in PEO-PPO-PEO system (see **Figure 6**), while gold nanoparticles with diameter of 10-30 nm were formed in PEO-PPO-NH_2 system in the temperature range 20-80 °C (see **Figure 7**).

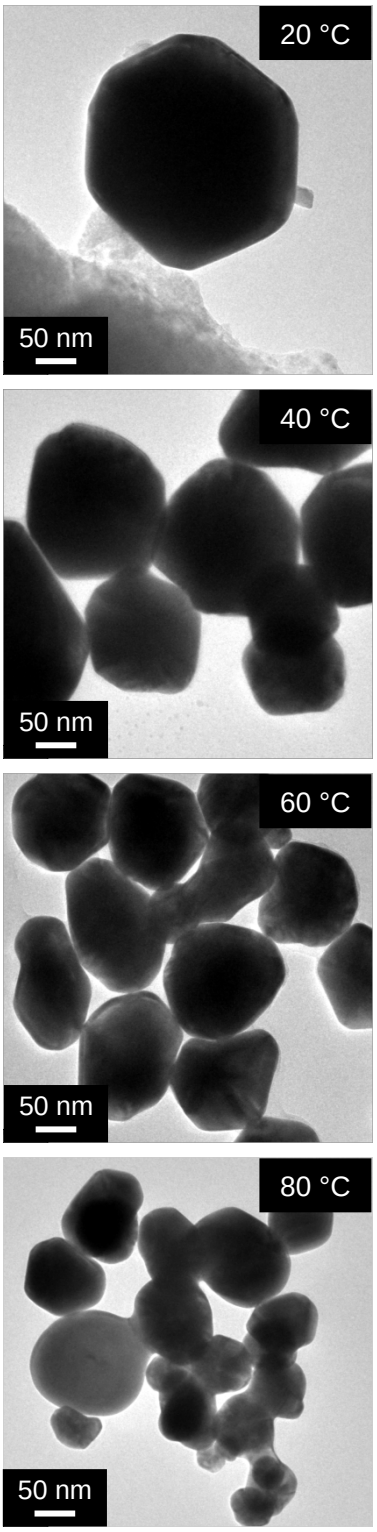

Figure 6. TEM images of gold particles formed in aqueous PEO-PPO-PEO solutions at 20 ˚C (for 348 h), 40 ˚C (for 150 h), 60 ˚C (for 8 h) and 80 ˚C (for 4 h).

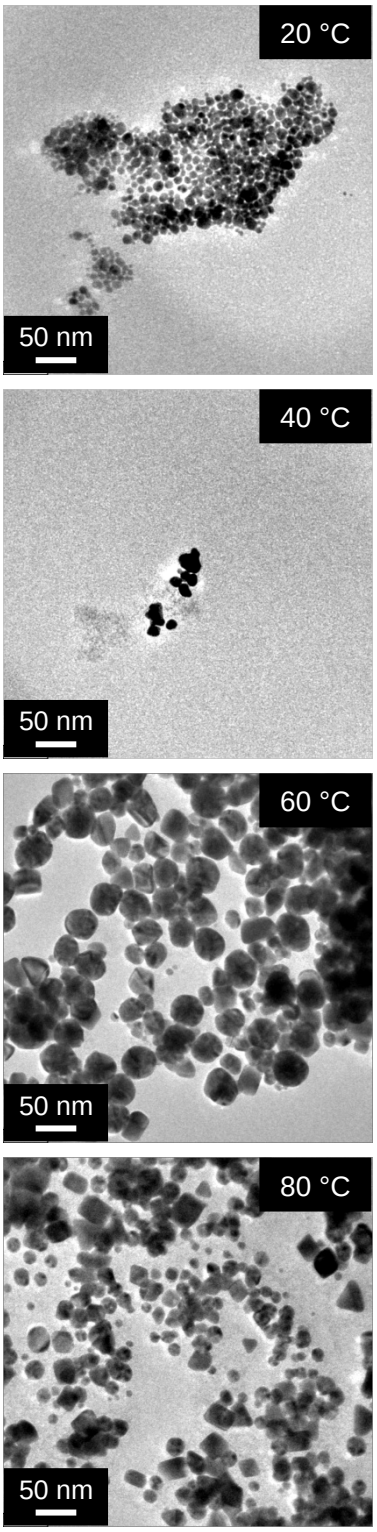

Figure 7. TEM images of gold particles formed in aqueous PEO-PPO-NH_2 solutions at 20 ˚C (for 480 h), 40 ˚C (for 360 h), 60 ˚C (for 240 h) and 80 ˚C (for 60 h).

In the case of PEO homopolymer, irregular-shaped gold particles with 20-800 nm containing polyhedral particles and elongated particles were formed in the temperature range 20-80 °C (see **Figure 8**). This would be attributed to the low interfacial activity of PEO homopolymer for gold surface. Formation of irregular-shaped gold particles with diameter ~500 nm and networks in PE-PEO system is also most likely due to the low interfacial activity of PE-PEO for gold surface (see **Figure 9**).

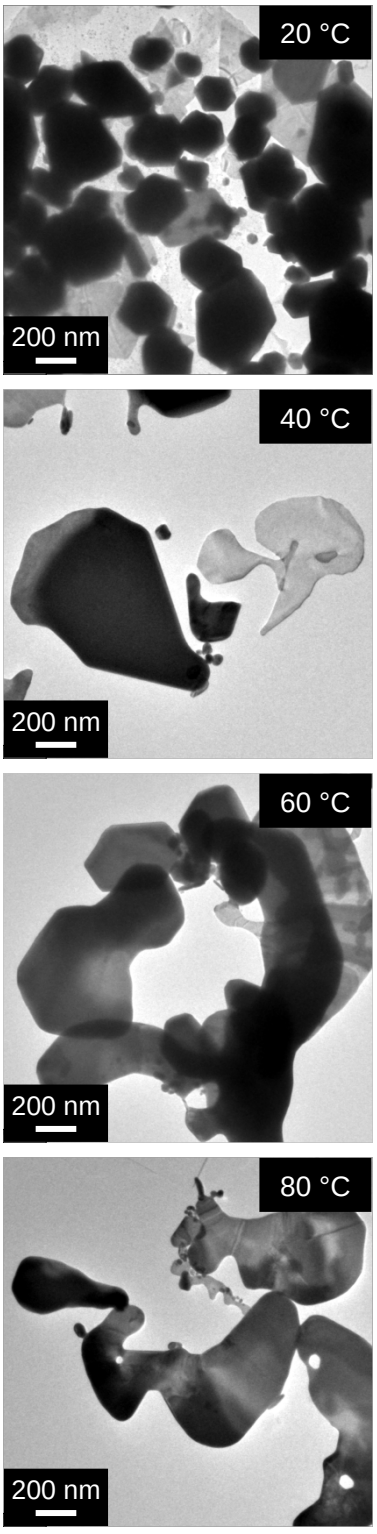

Figure 8. TEM images of gold particles formed in aqueous PEO solutions at 20 ˚C (for 408 h), 40 ˚C (for 96 h), 60 ˚C (for 20 h) and 80 ˚C (for 6 h).

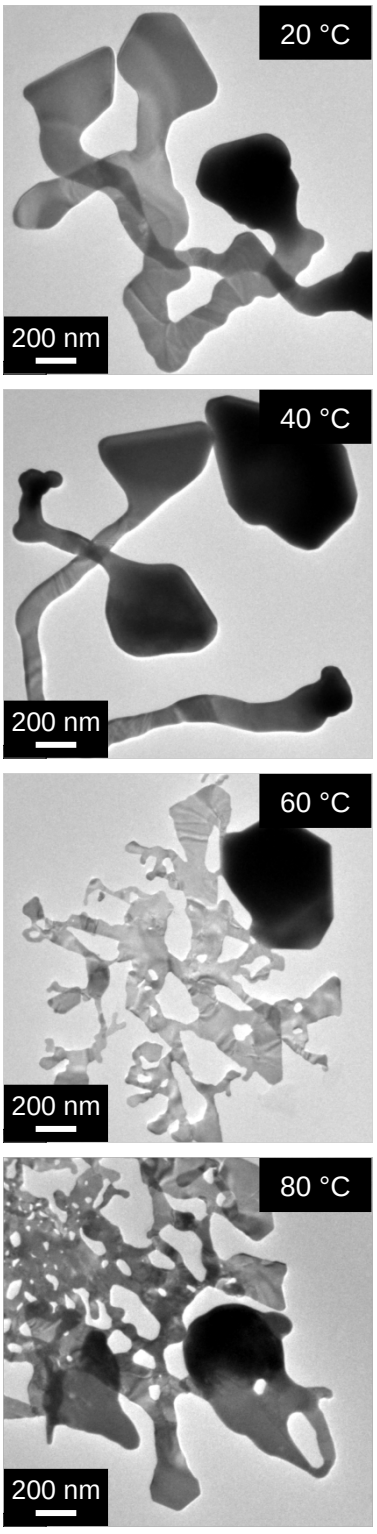

Figure 9. TEM images of gold particles formed in aqueous PE-PEO solutions at 20 ˚C (for 480 h), 40 ˚C (for 120 h), 60 ˚C (for 30 h) and 80 ˚C (for 12 h).

4.4 Effect of temperature on morphology of gold nanoparticles formed

As mentioned in section 4.3, the relationship between reduction activity and interfacial activity (affinity) of PEO-BCP determines the growth and final morphology of gold nanoparticles. In the case of PEO-PPO-PEO, large nanoparticles were formed (see **Figure 6**) because the $[AuCl_4]^-$ reduction on the gold seeds was enhanced by the synergistic effect of high reduction activity for $[AuCl_4]^-$ and relatively high interfacial activity of PEO-PPO-PEO for gold surface. On the other hand, in the case of PEO-PPO-NH_2, small nanoparticles were formed (see **Figure 7**) because the stabilization of gold nanoparticles by PEO-PPO-NH_2 would be more dominant than $[AuCl_4]^-$ reduction by PEO-PPO-NH_2 adsorbed on gold seeds due to the low reduction activity for $[AuCl_4]^-$ and high interfacial activity (affinity) for gold surface. Then, we finally check the effect of temperature on the particle morphology because the reduction activity and several properties of PEO-BCP (e.g., solubility, interfacial activity, micelle formation, micelle structure) are strongly affected by temperature [43-46]. Indeed, the gold nanoparticles formed in the aqueous PEO-PPO-PEO solutions became smaller with higher temperature (see **Figure 6**). This suggests that $[AuCl_4^-]$ reduction by PEO-PPO-PEO occurs in the bulk solution rather than on the surface of gold seeds at higher temperature. This is most likely due to desorption of PEO-PPO-PEO from the gold surface caused by increase in the thermal mobility. On the other hand, gold nanoparticles formed in the aqueous PEO-PPO-NH_2 solutions became larger as temperature elevation (see **Figure 7**). This suggests that the reduction of $[AuCl_4]^-$ by PEO-PPO-NH_2 adsorbed on gold seeds is enhanced by temperature elevation. This would be attributed to the synergistic effect of increase in the reduction activity by heating (see **Figure 3**) and the strong affinity of PEO-PPO-NH_2 for gold surface (see

Table 1). The morphology of gold particles formed in the PEO and PE-PEO systems does not seem to be affected by temperature (see **Figures 8 and 9**).

5. Conclusions

We have investigated in this work the connections between block copolymer segments (PEO, PPO, NH_2 and PE), reduction activity for $[AuCl_4]^-$, interfacial activity (affinity) of PEO-BCP for gold surface, stabilization of gold particles and morphology of gold particles formed. The reduction activity of PEO-BCP for $[AuCl_4]^-$ was enhanced in the presence of poly(propylene oxide) (PPO) segment in block copolymer. On the other hand, the $[AuCl_4]^-$ reduction was prevented by the amino group (NH_2) and hydrocarbon chain (PE). This is most likely attributed to (i) block copolymer conformation or structure (e.g., loops vs. entanglements, or non-associated polymers vs. micelles) and (ii) interactions between $AuCl_4^-$ ions and block copolymers (attractive ion-dipole interactions vs. repulsive interactions due to hydrophobicity). Since the reduction activity of PEO-PPO-PEO (which forms micelles) was higher than that of PEO homopolymer (which is non-associated polymer), it is suggested that micelle formation is related to the reduction activity of PEO-BCP for $[AuCl_4]^-$. The micelle corona composed of PEO would act as an appropriate reaction site for $[AuCl_4]^-$ reduction. Lower reduction activity of PEO-PPO-NH_2 and PE-PEO than that of PEO homopolymer suggests that strong hydrogen bonding among amino groups and repulsive interaction afforded by polymer hydrophobicity prevent the ion-dipole interaction between $[AuCl_4]^-$ and PEO-BCP. The interfacial activity (affinity) of PEO-PPO-NH_2 for gold surface was extremely high compared with PEO-PPO-PEO, PEO homopolymer and PE-PEO. As a result, high colloidal stability of gold

nanoparticles was achieved in the aqueous PEO-PPO-NH_2 solutions. Furthermore, the high interfacial activity (affinity) of PEO-PPO-NH_2 for gold surface prevented the particle growth, and consequently the smaller nanometer-sized gold particles were formed. These findings should provide insights and offer further opportunities on the synthetic strategy in the block copolymer-mediated synthesis of metal nanoparticles in solutions.

Acknowledgements

This study was performed through Program for Dissemination of Tenure Tracking System funded by the Ministry of Education and Science, Japan.

References

[1] M.C. Daniel, D. Astruc, Chem. Rev. 104 (2004) 293.

[2] S. Eustis, M.A. El-Sayed, Chem. Soc. Rev. 35 (2006) 209.

[3] C. Burda, X.B. Chen, R. Narayanan, M.A. El-Sayed, Chem. Rev. 105 (2005) 1025.

[4] J. Shan, H. Tenhu, Chem. Commun. (2007) 4580.

[5] Y.J. Xiong, Y.N. Xia, Adv. Mater. 19 (2007) 3385.

[6] J. Park, J. Joo, S.G. Kwon, Y. Jang, T. Hyeon, Angew. Chem. Int. Edit. 46 (2007) 4630.

[7] J. Sharma, T. Imae, J. Nanosci. Nanotechnol. 9 (2009) 19.

[8] J.F. Zhou, J. Ralston, R. Sedev, D.A. Beattie, J. Colloid Interface Sci. 331 (2009) 251.

[9] P.C. Ray, Chem. Rev. 110 (2010) 5332.

[10] A. Guerrero-Martinez, S. Barbosa, I. Pastoriza-Santos, L.M. Liz-Marzan, Curr. Opin. Colloid Interface Sci. 16 (2011) 118.

[11] M.B. Cortie, A.M. McDonagh, Chem. Rev. 111 (2011) 3713.

[12] M. Brust, M. Walker, D. Bethell, D.J. Schiffrin, R. Whyman, J. Chem. Soc.-Chem. Commun. (1994) 801.

[13] F. Dumur, A. Guerlin, E. Dumas, D. Bertin, D. Gigmes, C.R. Mayer, Gold Bull. 44 (2011) 119.

[14] P. Alexandridis, Chem. Eng. Technol. 34 (2011) 15.

[15] P. Alexandridis, M. Tsianou, Euro. Polym. J. 47 (2011) 569.

[16] M. Iwamoto, K. Kuroda, V. Zaporojtchenko, S. Hayashi, F. Faupel, Euro. Phys. J. D 24 (2003) 365.

[17] J.D.S. Newman, G.J. Blanchard, Langmuir 22 (2006) 5882.

[18] J.D.S. Newman, G.J. Blanchard, J. Nanoparticle Res. 9 (2007) 861.

[19] T. Sakai, M. Ishigaki, T. Okada, S. Mishima, J. Nanosci. Nanotechnol. 10 (2010) 919.

[20] T. Sakai, M. Ishigaki, T. Okada, S. Mishima, Chem. Lett. 40 (2011) 501.

[21] X.P. Sun, X. Jiang, S.J. Dong, E.K. Wang, Macromol. Rapid Commun. 24 (2003) 1024.

[22] Y.L. Luo, Mater. Lett. 61 (2007) 1039.

[23] S.F. Pang, T. Kondo, T. Kawai, Chem. Mater. 17 (2005) 3636.

[24] L. Longenberger, G. Mills, J. Phys. Chem. 99 (1995) 475.

[25] T. Sakai, P. Alexandridis, Langmuir 20 (2004) 8426.

[26] T. Sakai, P. Alexandridis, J. Phys. Chem. B 109 (2005) 7766.

[27] T. Sakai, P. Alexandridis, Langmuir 21 (2005) 8019.

[28] T. Sakai, P. Alexandridis, Chem. Mater. 18 (2006) 2577.

[29] T. Sakai, P. Alexandridis, Macromol. Symp. 289 (2010) 18.

[30] P. Khullar, A. Mahal, V. Singh, T.S. Banipal, G. Kaur, M.S. Bakshi, Langmuir 26 (2010) 11363.

[31] P. Khullar, V. Singh, A. Mahal, H. Kaur, V. Singh, T.S. Banipal, G. Kaur, M.S. Bakshi, J. Phys. Chem. C 115 (2011) 10442.

[32] T. Ishii, H. Otsuka, K. Kataoka, Y. Nagasaki, Langmuir 20 (2004) 561.

[33] S. Goy-Lopez, E. Castro, P. Taboada, V. Mosquera, Langmuir 24 (2008) 13186.

[34] J. Keilitz, M.R. Radowski, J.D. Marty, R. Haag, F. Gauffre, C. Mingotaud, Chem. Mater. 20 (2008) 2423.

[35] T. Sakai, T. Mukawa, K. Tsuchiya, H. Sakai, M. Abe, J. Nanosci. Nanotechnol.

9 (2009) 461.

[36] C.F. Bohren, D.R. Huffman, Absorption and Scattering of Light by Small Particles, Wiley, New York, 1983.

[37] S. Link, M.A. El-Sayed, J. Phys. Chem. B 103 (1999) 8410.

[38] A. Warshawsky, R. Kalir, A. Deshe, H. Berkovitz, A. Patchornik, J. Am. Chem. Soc. 101 (1979) 4249.

[39] B.J. Elliott, A.B. Scranton, J.H. Cameron, C.N. Bowman, Chem. Mater. 12 (2000) 633.

[40] S. Yanagida, K. Takahashi, M. Okahara, Bull. Chem. Soc. Jpn. 50 (1977) 1386.

[41] M.M. Bloomfield, Chemistry and the Living Organism, 5th Edition, John Wiley & Sons, Inc., New York, 1991.

[42] T. Sugimoto, Fine Particles-Synthesis, Characterization, and Mechanisms of Growth, Marcel Dekker, Inc., New York, 2000.

[43] P. Alexandridis, T. Nivaggioli, T.A. Hatton, Langmuir 11 (1995) 1468.

[44] Y.N. Lin, P. Alexandridis, J. Phys. Chem. B 106 (2002) 10834.

[45] P. Alexandridis, L. Yang, Macromolecules 33 (2000) 3382.

[46] L. Yang, P. Alexandridis, Langmuir 16 (2000) 4819.